Research Square

Preprints are preliminary reports that have not undergone peer review.
They should not be considered conclusive, used to inform clinical practice,
or referenced by the media as validated information.

Study on the Group Anchoring Effect of Retractable Anchor Cables and Parameter Analysis

Shuaihua Ye
Lanzhou University of Technology
Pengxu ZHANG
Lanzhou University of Technology
Liangliang XIN
liangliangxin2022@163.com
Lanzhou University of Technology
Bassam Z. Mahasneh
Mutah University
Jiaxuan ZHENG
Lanzhou University of Technology

Research Article

Keywords: Retrievable anchor cables, group anchoring effect, excavation engineering, additional force, group anchoring effect coefficient

Posted Date: November 10th, 2026

DOI: https://doi.org/10.21203/rs.3.rs-11375311/v1

License: This work is licensed under a Creative Commons Attribution 4.0 International License.
Read Full License

Additional Declarations: No competing interests reported.

Study on the Group Anchoring Effect of Retractable Anchor Cables and Parameter Analysis

YE Shuaihua[1]，ZHANG Pengxu[1]，XIN Liangliang[1] ,Bassam Z. Mahasneh[2] , ZHENG Jiaxuan[1]

(1. *School of Civil and Hydraulic Engineering，Lanzhou University of Technology，Lanzhou，Gansu* 730050，*China*；

2. *Civil and environmental engineering department，Mutah university，Al Karak, Karak Governorate 61710, Jordan*)

Abstruct: The group anchor effect of recoverable anchor cable directly affects the overall bearing capacity of foundation pit supporting structure, but there is no systematic quantitative analysis method at present. In this paper, the calculation model of bearing capacity of single recoverable anchor cable is constructed, and the calculation formula of bearing capacity is derived. Then, based on the actual arrangement of group anchors, the calculation model of additional force transfer of adjacent anchor cables in the upper, lower, left and right layers is established, and the formulas of additional force in each direction are derived, and the group anchor effect coefficient is used as the quantitative index. By comparing the theoretical calculation results of this paper with the theoretical and numerical simulation results of the existing literature, the rationality of the calculation method is verified. The results show that the group anchor effect coefficient increases with the increase of soil cohesion and anchor cable arrangement spacing, and decreases with the increase of anchor cable arrangement inclination, calculation of anchor cable anchorage section length and transmission anchor cable anchorage section length. The research results can provide theoretical support and quantitative basis for the design of recyclable anchor cable group.

Key words: Retrievable anchor cables; group anchoring effect; excavation engineering; additional force; group anchoring effect coefficient

1 Introduction

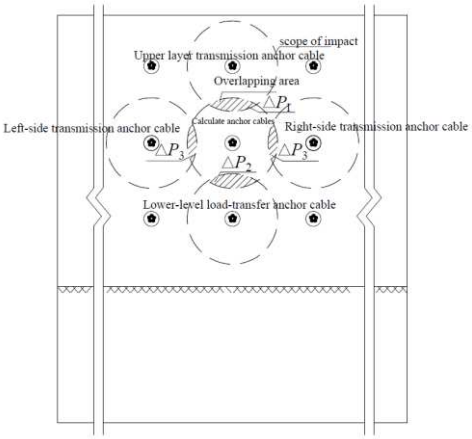
With the development of urban underground space in China to larger, deeper and more complex conditions, the scale and difficulty of deep foundation pit engineering continue to increase, and higher requirements are put forward for the anchorage bearing capacity, stability and economy of the support system [1-6]. Recyclable anchor cable [7-10] has been gradually popularized and applied in major projects such as foundation pit of large-scale high-rise building, underground pipe gallery and rail transit hub by virtue of its advantages of recyclable utilization, no underground residual pollution and adaptability to green construction concept. The ultimate pullout resistance and failure mechanism of single anchor cable have been preliminarily clarified [11-13]. However, in practical engineering, the bearing capacity of single anchor cable is often difficult to meet the anchoring requirements of large and complex deep foundation pit, and the anchor cables usually need to be densely arranged in the form of group anchors, which provide sufficient support resistance through the cooperation of multiple anchor cables, and the group anchor arrangement has become the mainstream form of recoverable anchor cable engineering application，The technical challenges arising from the group anchor effect are becoming increasingly prominent. For example: When multiple cables are densely arranged, the stress fields of adjacent cables overlap each other and the deformation of rock and soil coordinate with each other, which leads to uneven load

distribution in the cable group, early failure of some cables due to overload, and significant reduction of overall anchoring efficiency. At present, scholars have made certain research progress and fruitful achievements in the research of anchor group effect. Pei Yajian [14] gave a calculation method of anchor group effect coefficient on the basis of improving the shear stress of central anchor cable and considering the stress superposition of surrounding anchor cables; Lu Ruina [15] deduced the pull-out bearing capacity of single anchor rod and anchor group effect coefficient on the basis of anchor group failure mechanism and pile group method, and proposed increasing burial depth to reduce anchor group effect. Both of them aim at quantifying group anchor action and improve anchor structure calculation system. Chen Chen et al.[16] found through group anchor pull-up model test of continuous spherical enlarged anchor that the influence range of soil displacement in elastic stage is the largest when shallow buried, and the influence range of displacement in elastoplastic stage is the largest when deep buried, and the incremental displacement first expands and then contracts. Pang Youshi et al.[17] showed that group anchor effect is significantly affected by rock and soil properties, and the influence of anchor spacing in rock mass is small, and the influence in soil layer is large. Ghaly[18] and Hanna[19] obtained from the screw anchor test in sand that the pullout performance of the group anchor depends on the diameter, burial depth, spacing, sand strength and embedding process. Huang Hongyang [20] combined the group anchor pullout test and numerical simulation to analyze the influence of burial depth and anchor spacing on the anchor body. Qiao Jiangang et al.[21] established the pullout bearing capacity model and discrete element model of the anti-floating anchor, and found that when the anchor pile spacing is 4D, 6D, and 8D, the axial and shear stresses first increase and then decrease and tend to be stable. In order to quantitatively analyze the anchor group effect of recoverable anchor cables, a bearing capacity calculation model of single recoverable anchor cable is established and its bearing capacity calculation formula is deduced. Based on the calculation model of cable bearing capacity and the actual arrangement of group anchors in foundation pit engineering, the calculation models of additional force transfer between upper layer, lower layer, left side and right side adjacent cables are established respectively, and the calculation formulas of additional force in each direction are deduced, and the group anchor effect coefficient is taken as the quantitative index of group anchor effect. Finally, the influence of soil cohesion, cable spacing, cable inclination and cable anchorage length on the group anchor effect coefficient is discussed.

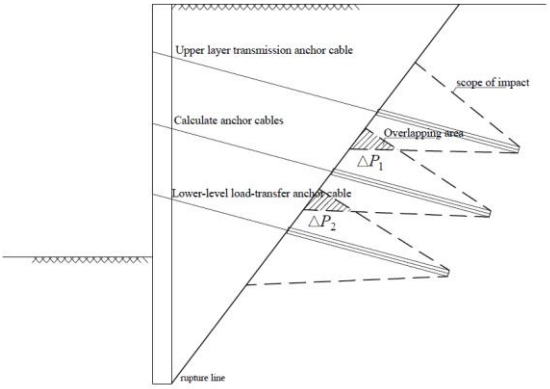
2 Group anchor effect of recoverable anchor cable

The anchor group effect is that multiple recyclable anchor cables are arranged at a certain spacing. After being tensioned, the stress fields of the individual anchor cables overlap and affect each other, making the stress

state of the soil in the anchorage zone significantly different from that of the individual anchor cables acting independently. Figure 1 (a-b) is a schematic diagram of the anchor group effect of recyclable anchor cables.



（a）elevation



（b）profile map

Fig. 1 Schematic diagram of anchor group effect of recoverable anchor cable

In Figure 1 (a-b), ΔP_1、ΔP_2 and ΔP_3 are the partial weakening of the upper, lower, left and right transfer cables to the calculated cable capacity, respectively. Taking three rows of recoverable anchor cables as an example, if one recoverable anchor cable is selected as the research object (calculation anchor cable), other recoverable anchor cables (transfer anchor cable) will be arranged horizontally and vertically, and the mechanical action of the transfer anchor cable will weaken the bearing capacity of the calculation anchor cable.The total weakening amount is the superposition value of the partial weakening amounts ΔP_1、ΔP_2 and $2\Delta P_3$. In order to calculate the effective bearing capacity of recoverable anchor cable under the influence of anchor group effect, it is necessary to consider the additional forces transmitted by adjacent cables on the upper side, lower side, left side and right side of the anchor cable, and carry out classified discussion.

3 Calculation model of group anchor effect of recoverable anchor cable

3.1 Calculation model of bearing capacity of single recoverable anchor cable

Before calculating the bearing capacity of recoverable anchor cable under the effect of anchor group, the force analysis of single anchor cable shall be done：

(1) Assuming that the angle between the fracture line of homogeneous soil layer and the horizontal line of ground is 45°+φ/2, the soil resistance and tensile strength outside the fracture plane are not considered;

(2) Because there is a certain inclination angle in the layout of recoverable anchor cable, the fracture plane shape of recoverable anchor cable is assumed to be irregular awl shape;

(3) Ignoring the influence of anchor body diameter of recoverable anchor cable;

(4) Assuming that the lateral pressure coefficient of soil is 1, the recoverable anchor cable is in hydrostatic pressure state;

(5) Assuming that the fracture angle is θ, according to relevant data [15, 22], θ is between 30° and 40 °.

The calculation model of bearing capacity of single recoverable anchor cable is shown in Figure 2. where ***P*** is the bearing capacity of the anchor cable, ***H*** is the distance from the bottom of the anchor cable to the ground, ***σ*** is the normal stress at the fracture surface, ***τ*** is the shear stress at the fracture surface, h_1 is the length of the free section of the anchor cable, h_2 is the length of the anchor cable, **A** is the bottom of the anchor cable, **B** is the intersection of the fracture surface at the lower part of the anchor cable and the fracture line, **C** is the intersection of the fracture surface at the upper part of the anchor cable and the fracture line, and **O** is the boundary point between the anchor cable and the free section.

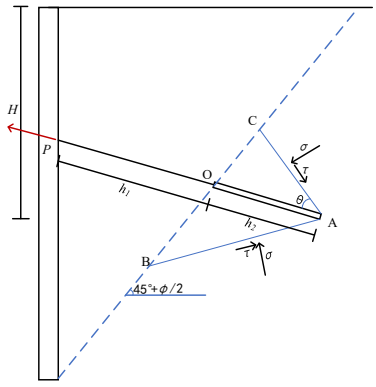


Fig. 2 Calculation Diagram of Failure of Single Anchor Cable

The stress along the recoverable cable axis at the fracture plane is：

$$\tau = -\gamma H \sin\theta + \left(\gamma H \tan\varphi + c\right)\cos\theta \tag{1}$$

In equation (1), γ is soil weight, c is soil cohesion, φ is soil internal friction angle.

The fracture plane shape of the cable is developed laterally and configured as a regular fan, as shown in Figure 3, where L_1 is the length of AB, L_2 is the length of AC, δ is the angle of the fan, and l is the chord length of the fan.

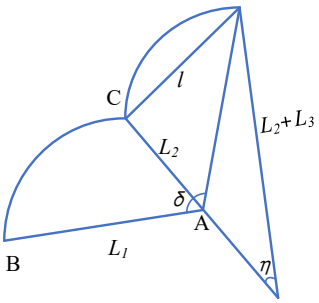


Fig. 3 Schematic Diagram of Regular Sector of Fracture Surface Structure

The projection radius can be expressed as $L_1 sin\theta$, δ can be expressed as $\pi \sin\theta$, l can be obtained by cosine theorem:

$$l = \sqrt{L_1^2 + L_2^2 - 2L_1L_2\cos(\delta/2)} \tag{2}$$

From the sine theorem:

$$\frac{l}{\sin(\delta/2)} = \frac{L_1}{\sin(90^\circ - \eta/2)} = \frac{L_2}{\sin(90^\circ + \eta/2 - \delta/2)} \tag{3}$$

$$\frac{l}{\sin\eta} = \frac{L_2 + L_3}{\cos(\eta/2)} \tag{4}$$

From equations (3) and (4), equations (5) and (6) can be obtained:

$$\eta = 2\arccos\left[\frac{L_1\sin(\delta/2)}{l}\right] \tag{5}$$

$$L_3 = \frac{l}{2\sin\eta(\eta/2)} - L_2 \tag{6}$$

Sector area S is:

$$S = \eta(L_2 + L_3)^2 - L_3(L_2 + L_3)^2\sin\eta \tag{7}$$

In this case, the bearing capacity of the recoverable anchor cable can be obtained from Equation (8):

$$P = \left[-\gamma H\sin\theta + (\gamma H\tan\theta + c)\cos\theta\right] \cdot\left[\eta(L_2 + L_3)^2 - L_3(L_2 + L_3)^2\sin\eta\right] \tag{8}$$

3.2 Calculation model of additional force transmitted by recoverable anchor cable in upper layer

If adjacent retrievable cables are used to calculate the distance H_1 above the cable, the calculation model is shown in Figure 4 below. where ***P*** is the bearing capacity of the anchor cable, the anchor cable layout inclination angle is ***α***, the fracture surface angle is ***θ***, ***H*** is the distance from the bottom end point of the anchor cable

anchoring section to the ground, h_1 is the length of the free section of the anchor cable, h_2 is the length of the anchor cable anchoring section, ***A*** is the bottom end point of the anchor cable, ***B*** is the intersection point of the fracture surface and the fracture line at the lower part of the anchor cable, ***C*** is the intersection point of the fracture surface and the fracture line at the upper part of the anchor cable, and O is the boundary point between the anchor cable anchoring section and the free section., p_1 is the average stress transmitted from the upper anchor cable to the fracture plane of the calculation anchor cable, l_0 is the distance from the overlapping area **I** constructed to the fracture line, h_3 is the length of the free section of the upper transmission anchor cable, h_4 is the length of the anchoring section of the upper transmission anchor cable, **D** is the bottom point of the transmission anchor cable, **E** is the intersection point of the fracture plane and the fracture line at the upper transmission anchor cable, **H** is the intersection point of the fracture plane and the fracture line at the lower part of the upper transmission anchor cable, **F** is the boundary point between the anchoring section and the free section of the upper transmission anchor cable, **I, C, H** is the intersection of two fracture planes.。

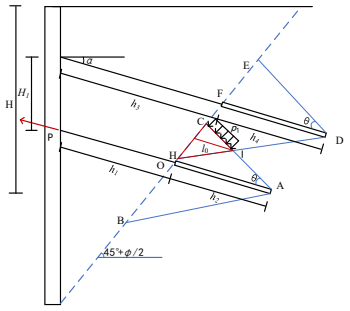


Figure 4 Calculation model of load transfer of upper layer anchor cable

Assuming that the fracture range of each cable is similar, there is：

$$\angle EFD = \angle COA = 45^\circ + \varphi/2 + \alpha$$

$$\angle FHD = \angle OBA = 45^\circ + \varphi/2 + \alpha - \theta$$

$$\angle HFD = \angle BOA = 135^\circ - \varphi/2 - \alpha$$

$$\angle FED = \angle OCA = 135^\circ - \varphi/2 - \alpha - \theta$$

In △COA and △EFD the sine theorem gives：

$$\begin{cases} \dfrac{h_2}{\sin\left(135^\circ - \varphi/2 - \theta - \alpha\right)} = \dfrac{OC}{\sin\theta} = \dfrac{AC}{\sin\left(45^\circ + \varphi/2 + \alpha\right)} \\ \dfrac{h_4}{\sin\left(135^\circ - \varphi/2 - \theta - \alpha\right)} = \dfrac{FE}{\sin\theta} = \dfrac{DE}{\sin\left(45^\circ + \varphi/2 + \alpha\right)} \end{cases} \quad (9)$$

From equation（9）we obtain：

$$\begin{cases} OC = h_2 \sin\theta / \sin\left(135^\circ - \varphi/2 - \theta - \alpha\right) \\ AC = \dfrac{h_2 \sin\left(45^\circ + \varphi/2 + \alpha\right)}{\sin\left(135^\circ - \varphi/2 - \theta - \alpha\right)} \\ FE = h_4 \sin\theta / \sin\left(135^\circ - \varphi/2 - \theta - \alpha\right) \\ DE = \dfrac{h_4 \sin\left(45^\circ + \varphi/2 + \alpha\right)}{\sin\left(135^\circ - \varphi/2 - \theta - \alpha\right)} \end{cases} \tag{10}$$

The same can be said：

$$\begin{cases} OB = h_2 \sin\theta / \sin\left(45^\circ + \varphi/2 + \alpha - \theta\right) \\ AB = \dfrac{h_2 \sin\left(135^\circ - \varphi/2 - \alpha\right)}{\sin\left(45^\circ + \varphi/2 + \alpha - \theta\right)} \\ FH = h_4 \sin\theta / \sin\left(45^\circ + \varphi/2 + \alpha - \theta\right) \\ HD = \dfrac{h_4 \sin\left(135^\circ - \varphi/2 - \alpha\right)}{\sin\left(45^\circ + \varphi/2 + \alpha - \theta\right)} \end{cases} \tag{11}$$

Figure 3.3 shows：

$$\begin{cases} OF = H_1 \cos\alpha / \sin\left(45^\circ + \varphi/2 + \alpha\right) \\ BC = h_2 \sin\theta / \sin\left(45^\circ + \varphi/2 + \alpha - \theta\right) \\ \quad + h_2 \sin\theta / \sin\left(135^\circ - \varphi/2 - \alpha - \theta\right) \\ HE = h_4 \sin\theta / \sin\left(45^\circ + \varphi/2 + \alpha - \theta\right) \\ \quad + h_4 \sin\theta / \sin\left(135^\circ - \varphi/2 - \alpha - \theta\right) \end{cases} \tag{12}$$

CHI for the overlapping part of the two fracture planes, i.e., the transmission part of the calculation cable, the calculation idea is the same as that of single cable calculation，Let IH length be L_4，IC length be L_5，In △CHI，we can obtain by sine theorem：

$$\frac{CH}{\sin 2\theta} = \frac{L_4}{\sin\left(135^\circ - \dfrac{\varphi}{2} - \theta - \alpha\right)} = \frac{L_5}{\sin\left(45^\circ + \dfrac{\varphi}{2} + \alpha - \theta\right)} \tag{13}$$

In equation (13)，CH=OC+FH-OF，all lengths have been derived. From equation (13), we can obtain：

$$\begin{cases} L_4 = \dfrac{\sin\left(135^\circ - \varphi/2 - \theta - \alpha\right) \cdot CH}{\sin 2\theta} \\ L_5 = \dfrac{\sin\left(45^\circ + \varphi/2 + \alpha - \theta\right) \cdot CH}{\sin 2\theta} \end{cases} \tag{14}$$

The following results are obtained by applying the same regular sector structure to the overlapping part：

$$\eta_1 = 2\arccos\left[\frac{L_4 \sin\left(\delta_1/2\right)}{l_1}\right] \tag{15}$$

$$L_6 = \frac{l_1}{2\sin\eta_1\left(\eta_1/2\right)} - L_5 \tag{16}$$

The overlapping sector area S_1 is：

$$S_1 = \eta_1\left(L_5 + L_6\right)^2 - L_6\left(L_5 + L_6\right)^2 \sin\eta_1 \tag{17}$$

Assuming that the forces transmitted by the upper cable to the calculated cable are uniformly distributed, the average stress p_1 is：

$$p_1 = \frac{1}{2}\left(p_{l_0} + p_0\right) \tag{18}$$

In equation（18）, p_{l_0} and p_0 are the stresses transmitted at the beginning of the cable and to the fracture plane, respectively.

$$\begin{cases} p_{l_0} = \dfrac{P}{\pi\left(h_4 - l_0\right)^2 \tan\theta \cdot HE/2h_4} \\ p_0 = \dfrac{P}{\pi h_4 \tan\theta \cdot HE/2} \end{cases} \tag{19}$$

in equation (19) can be obtained from the similarity relation.

Therefore, the shear stress transmitted by the upper cable along the cable axis can be expressed as：

$$\tau_1 = p_1 \cdot \left(1 - \sin\theta\cos\theta\tan\varphi\right) \tag{20}$$

From equations (20) and (17), the additional force ΔP_1 transmitted by the upper anchor cable can be obtained as:

$$\begin{aligned} \Delta P_1 = \tau_1 \cdot S_1 = &\left[p_1 \cdot \left(1 - \sin\theta\cos\theta\tan\varphi\right)\right] \\ &\cdot\left[\eta_1\left(L_5 + L_6\right)^2 - L_6\left(L_5 + L_6\right)^2 \sin\eta_1\right] \end{aligned} \tag{21}$$

3.3 Calculation model of additional force transmitted by recoverable anchor cable in lower layer

When the retrievable anchor cable transmitted is used to calculate the distance of H_2 under the anchor cable, the calculation model is shown in Figure 5 below.

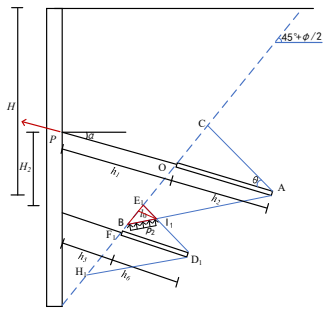


Fig. 5 Calculation Model of Load Transfer of Lower Anchor Cable

Where P is the anchor cable bearing capacity, Anchor cable laying inclination is α, The fracture plane angle is θ, H is the distance from the bottom point of the anchor cable anchoring section to the ground, h_1 is the length of the free section of the anchor cable, h_2 is the length of the anchor cable anchoring section, A is the bottom point of the anchor cable anchoring section, B is the intersection point of the fracture plane and the fracture line at the lower part of the anchor cable anchoring section, C is the intersection point of the fracture plane and the fracture line at the upper part of the anchor cable anchoring section, O is the boundary point between the anchor cable anchoring section and the free section, p_2 is the average stress transmitted from the lower anchor cable to the fracture plane of the calculation anchor cable, l_0 is the distance from the overlapping area $\mathbf{I_1}$ constructed to the fracture line, h_5 is the length of the free section of the lower transmission anchor cable, h_6 is the length of the anchoring section of the lower transmission anchor cable, $\mathbf{D_1}$ is the bottom point of the lower transmission anchor cable, E_1 is the intersection of the fracture plane and the fracture line at the upper part of the lower transmission anchor cable, $\mathbf{H_1}$ is the intersection of the fracture plane and the fracture line at the lower part of the lower transmission anchor cable, $\mathbf{F_1}$ is the boundary point between the anchoring section and the free section of the lower transmission anchor cable, $\mathbf{I_1}$, $\mathbf{B}$, $\mathbf{E_1}$ is the intersection of two fracture planes.

Assuming that the fracture range of each cable is similar, there is

$$\angle E_1F_1D_1 = \angle COA = 45^\circ + \varphi/2 + \alpha$$

$$\angle F_1H_1D_1 = \angle OBA = 45^\circ + \varphi/2 + \alpha - \theta$$

$$\angle H_1F_1D_1 = \angle BOA = 135^\circ - \varphi/2 - \alpha$$

$$\angle F_1E_1D_1 = \angle OCA = 135^\circ - \varphi/2 - \alpha - \theta$$

OC、AC、AB and BO can be obtained from equations (10) and (11)，E_1F_1、E_1D_1、F_1H_1 and H_1D_1 can be derived from sine theorem：

$$\begin{cases} E_1D_1 = \dfrac{h_6 \sin\left(45^\circ + \varphi/2 + \alpha\right)}{\sin\left(135^\circ - \varphi/2 - \theta - \alpha\right)} \\ E_1F_1 = h_6 \sin\theta / \sin\left(135^\circ - \varphi/2 - \theta - \alpha\right) \\ F_1H_1 = h_6 \sin\theta / \sin\left(45^\circ + \varphi/2 + \alpha - \theta\right) \\ H_1D_1 = \dfrac{h_6 \sin\left(135^\circ - \varphi/2 - \alpha\right)}{\sin\left(45^\circ + \varphi/2 + \alpha - \theta\right)} \end{cases} \tag{22}$$

Figure 4 shows the geometric relationship：

$$\begin{cases} OF_1 = H_2 \cos\alpha / \sin\left(45^\circ + \varphi/2 + \alpha\right) \\ H_1E_1 = h_6 \sin\theta / \sin\left(45^\circ + \varphi/2 + \alpha - \theta\right) \\ \qquad + h_6 \sin\theta / \sin\left(135^\circ - \varphi/2 - \alpha - \theta\right) \end{cases} \tag{23}$$

BE_1I_1 is the overlapping part of two fracture planes, i.e. the transmission part of the calculation cable. The calculation idea is the same as above. Let I_1B have length L_7 , I_1E_1 have length L_8. In $\triangle BE_1I_1$, the sine theorem gives:

$$\begin{cases} L_7 = \sin\left(135^\circ - \varphi/2 - \theta - \alpha\right) \cdot BE_1 / \sin 2\theta \\ L_8 = \sin\left(45^\circ + \varphi/2 + \alpha - \theta\right) \cdot BE_1 / \sin 2\theta \end{cases} \tag{24}$$

In formula（24），$BE_1=E_1F_1+BO-OF_1$，each length has been derived.

The same can be obtained，

$$\eta_2 = 2\arccos\left[\frac{L_7 \sin\left(\delta_2/2\right)}{l_2}\right] \tag{25}$$

$$L_9 = \frac{l_2}{2\sin\eta_2\left(\eta_2/2\right)} - L_8 \tag{26}$$

The overlapping sector area S_2 is：

$$S_2 = \eta_2\left(L_8 + L_9\right)^2 - L_9\left(L_8 + L_9\right)^2 \sin\eta_2 \tag{27}$$

Average stress p_2 is：

$$p_2 = \frac{1}{2}\left(p_{l_0} + p_0\right) \tag{28}$$

In formula （28）：

$$\begin{cases} p_{l_0} = \dfrac{P}{\pi\left(h_6 - l_0\right)^2 \tan\theta \cdot H_1E_1 / 2h_6} \\ p_0 = \dfrac{P}{\pi h_6 \tan\theta \cdot H_1E_1 / 2} \end{cases}$$

Therefore, the shear stress transmitted by the lower cable is：

$$\tau_2 = p_2 \cdot \left(1 - \sin\theta\cos\theta\tan\varphi\right) \tag{29}$$

From equations (29) and (27), The additional force ΔP_2 transmitted by the upper anchor cable is：

$$\begin{aligned} \Delta P_2 = \tau_2 \cdot S_2 = &\left[p_2 \cdot \left(1 - \sin\theta\cos\theta\tan\varphi\right)\right] \\ &\cdot\left[\eta_2\left(L_8 + L_9\right)^2 - L_9\left(L_8 + L_9\right)^2 \sin\eta_2\right] \end{aligned} \tag{30}$$

3.4 Calculation model of additional force transmitted by left and right recyclable anchor cables

When the distance between the transferred recoverable anchor cable and the left or right side of the calculated

anchor cable is H_3, take the transferred anchor cable arranged on the right side of the calculated anchor cable as an example, make a section along the plane where the anchor cable is located and only reserve the fracture area of the anchor cable segment. See Figure 6 for the calculation model diagram.(The vertical profile is the same as Figure 2 since the retrievable cables are arranged at the same height horizontally.) where P is the cable bearing capacity, A is the bottom point of the cable, G is the intersection of the fracture plane at the left part of the cable and the plane section, K is the intersection of the fracture plane at the right part of the cable and the plane section, O is the boundary point between the anchor section and the free section of the cable, p_3 is the average stress transmitted from the right cable to the side of the fracture cone of the cable, A_1 is the bottom point of the cable transmitted from the right side, G_1 is the intersection of the fracture plane at the left part of the cable transmitted from the right side and the fracture line, K_1 is the intersection point of fracture plane and fracture line at the lower part of right transfer anchor cable, O is the boundary point between anchorage section and free section of right transfer anchor cable, I_3, K and G_1 are the intersection points of two fracture planes. Generally, the length of anchorage section of recoverable anchor cable arranged horizontally is the same, so the length of anchorage section of two anchor cables is h_7.

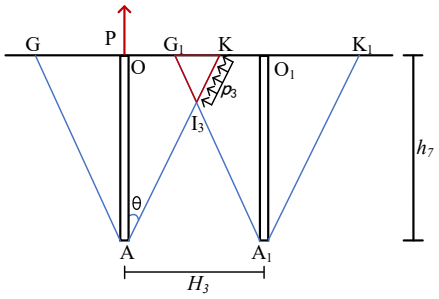


Fig. 6 Calculation Model for Load Transfer of Right Anchor Cable

Since the lengths of the anchor segments of recoverable cables arranged horizontally are generally the same, the approximate radius of the bottom circle of the fracture cone is $R = h_7 \tan\theta$， the bottom arc length of the stack is $2R\arccos(H_3^2 / 2RH_3)$。Since the area S3 of the upper superimposed portion cannot be accurately calculated, the radius of the expansion sector is $[(2R - H_3) / 2\sin\theta]$。

$$S_3 = R\arccos\frac{H_3^2}{2RH_3}\cdot\frac{2R - H_3}{2\sin\theta} \tag{31}$$

Average stress p_3 is：

$$p_3 = \frac{1}{2}\left(p_{l_0} + p_0\right) \tag{32}$$

In formula (32)：

$$\begin{cases} p_{l_0} = \dfrac{2P}{\pi h_7^{\,2} \tan\theta\left(G_1 K_1 / h_7\right)} \\ p_0 = \dfrac{2P}{\pi h_7 \tan\theta G_1 K_1} \end{cases}$$

Therefore, the shear stress transmitted by the right-hand cable is：

$$\tau_3 = p_3 \cdot \left(1 - \sin\theta\cos\theta\tan\varphi\right) \tag{33}$$

From equations (33) and (31), the additional force ΔP_3 transmitted by the upper anchor cable can be obtained as：

$$\Delta P_3 = \tau_3 \cdot S_3 = \left[p_3 \cdot \left(1 - \sin\theta\cos\theta\tan\varphi\right)\right] \cdot R \arccos\frac{H_3^2}{2RH_3} \cdot \frac{2R - H_3}{2\sin\theta} \tag{34}$$

3.5 Group anchor effect coefficient

At this time, the calculation formula for calculating the actual effective pullout bearing capacity of the anchor cable should be revised as：

$$P' = P - \Delta P_1 - \Delta P_2 - 2\Delta P_3 \tag{35}$$

In equation (35),P' is the effective bearing capacity of anchor cable calculated under group anchor arrangement; P is the bearing capacity of single recoverable anchor cable.

At present, in the current codes of engineering field, the key measure of controlling anchor group effect is adjusting the interval between adjacent anchor cables, and the related parameters are mostly given based on engineering experience, and the systematic theoretical derivation of the action mechanism and quantitative method of anchor group effect has not been carried out, which is difficult to meet the refined design requirements of new support components such as recoverable anchor cables, and only empirical values are easy to lead to design redundancy or insufficient safety reserve. Therefore, it is necessary to carry out quantitative analysis and research on anchor group effect of recoverable anchor cable. In order to directly characterize the influence degree of anchor group effect on pullout bearing capacity of recoverable anchor cable, anchor group effect coefficient psi is defined as the ratio of effective pullout bearing capacity P' of anchor cable calculated under anchor group arrangement to pullout bearing capacity P of single recoverable anchor cable. The calculation formula is as follows：

$$\psi = \frac{P'}{P} \tag{36}$$

The calculation result range of group anchor effect coefficient ψ should be [0，1]. The closer the result is to 1,

the weaker the interaction between group anchors is, and the pullout bearing capacity of recoverable anchor cable can be fully utilized. Otherwise, the stronger the interaction between group anchors is, and the pullout bearing capacity of single recoverable anchor cable is obviously weakened.

4 Example Analysis and Verification

4.1 project overview

The recoverable anchor cable groups of the foundation pit engineering are all embedded in the loess layer, with soil cohesion of 16.2kPa and heavy weight of 16.9kN/m3; the anchor cables are arranged in 3 rows and 3 columns; the horizontal spacing and vertical spacing are both 1.5m; The total length of the first and third rows of anchor cables is 10m, the anchor section is 5m, and the free section is 5m; the total length of the second row of anchor cables is 8m, the anchor section is 3m, and the free section is 5m; the anchor cable diameter is 150mm, and the layout inclination is 15°. The parameters for comparative analysis of various methods are selected from the project profile data.

4.2 numerical modeling

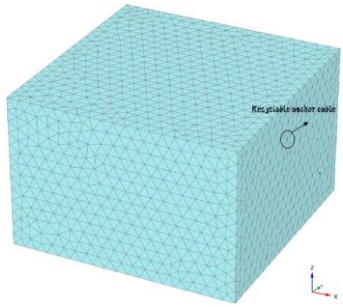
PLAXIS3D numerical simulation software is used to establish a recoverable anchor cable group anchor pulling model, and the values of model simulation parameters are shown in Table 1.

Table 1 Model simulation parameters

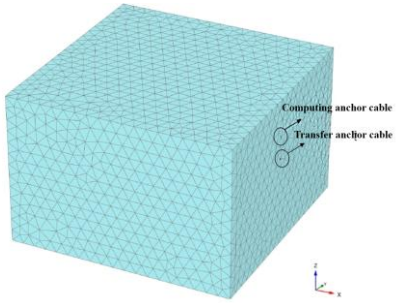
soil layer	severe kN/m^3	cohesive force kPa	internal friction angle °	elasticity modulus Mpa
loess	16.9	16.2	22.0	7.7

The anchor cable is calculated to be arranged at an inclination of 15°, with a total length of 8m, in which the length of the anchor section is 3m and the length of the free section is 5m. The model size is 15m×10m×10m. Meanwhile, the calculation models of recoverable anchor cables affected by different parts such as upper layer, lower layer and right side are established respectively to verify the rationality of each calculation model. The transmission anchor cables are all arranged at an inclination of 15°, with a total length of 10m, wherein the anchor section is 5m long and the free section is 5m long, which are respectively arranged at the upper layer 1.5 m, the lower layer 1.5 m and the right side 1.5 m of the calculation anchor cable. The mesh size is divided into fine, generating 18794 units and 29016 nodes, as shown in Figure 7 (a-d) below. Mohr-Coulomb strength criterion [23] is adopted for soil constitutive model, point-to-point anchor element is adopted for free section of anchor cable, embedded beam element is adopted for anchorage section, and boundary conditions of model are as follows:

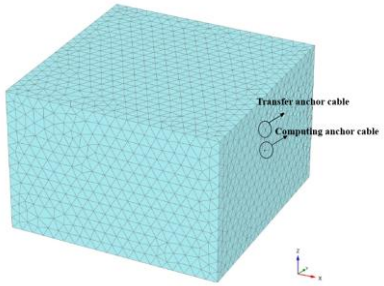
bottom surface is completely fixed, side surface is normally fixed, and top surface is free boundary.



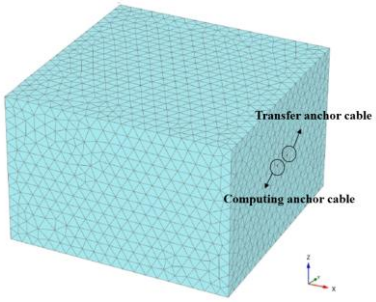
（a）Drawing Diagram of Single Anchor Cable



（b）Schematic Diagram of Group Anchor Pulling for Lower Anchor Line Transmission



（c）Schematic diagram of upper layer anchor cable transferring anchor group pulling

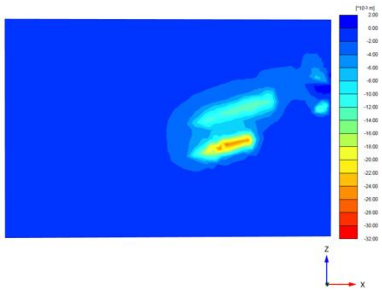


（d）Schematic Diagram of Right Anchor Cable Transfer Group Anchor Pulling

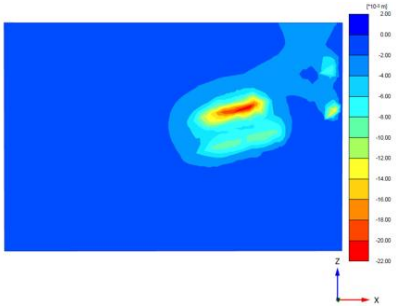
Fig. 7 Grid division diagram

Take the vertical section at 7m in y direction of transfer anchor group model in lower layer and upper layer, and you can see the displacement nephogram of maximum bearing capacity of anchor cable, as shown in Figure 8 (a-b). Take the transverse section at 5.5m in z direction of transfer anchor group model in right layer, you can see

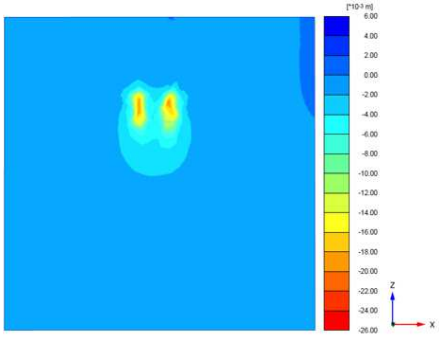
the displacement nephogram when calculating maximum bearing capacity of anchor cable, as shown in Figure 8 (c). From the simulation results, it can be seen that the failure mode is basically consistent with the change of theoretical calculation model, which fully proves the rationality of theoretical calculation model in this paper. The calculation method of numerical simulation anchor cable bearing capacity is to apply load step by step. When the load continues to rise, the model solution does not converge, and the displacement continues to develop and cannot converge to the stable state, so it is judged that the structure reaches the critical state of instability failure. According to the judgment principle of numerical simulation limit load, the load value calculated stably at the previous level before instability is taken as the bearing capacity [24]. The anchor cable is arranged in layers according to this method to calculate the bearing capacity, and the ratio thereof is taken as the group anchor effect coefficient in numerical simulation.



（a）Displacements of anchor groups transmitted by lower layer cables



（b）Displacements of anchor groups transmitted by upper cables



（c）Right anchor cable transmits displacement nephogram of anchor group

Figure 8 Cloud map of anchor group displacement

4.3 Comparative analysis

In order to verify the rationality of the calculation method of group anchor effect coefficient in this paper, the theoretical calculation method in literature [14] and the numerical simulation calculation results in this paper are used to compare with the calculation method proposed in this paper. See Table 2 for the results.

Table 2 Calculation results of anchor group effect coefficient of recoverable anchor cable

computing method / arrangement	Literature Methods [14]	numerical modeling	the proposed method
superstratum	0.873	0.804	0.847
lower layer	0.846	0.781	0.821
offside	0.862	0.793	0.835

It can be seen from Table 2 that the anchor group effect coefficient of recoverable anchor cable calculated by this method is very close to the calculation results of existing theory and numerical simulation. The anchor group effect coefficient of upper anchor cable after transmission is 2.6% smaller than that of original method and 4.3% larger than that of numerical simulation; the anchor group effect coefficient of lower anchor cable after transmission is 2.5% smaller than that of original method and 4.0% larger than that of numerical simulation; The group anchor effect coefficient after the right anchor cable transmission is 2.7% smaller than that of the original method and 4.2% larger than that of numerical simulation, and the reason why the calculation results in this paper are smaller than those of the original literature is that the parameters considered in the literature are not comprehensive, so the calculation results of group anchor effect are too conservative, and the group anchor effect coefficient is larger. The reason why the theoretical calculation results are larger than the numerical simulation results is that the basic assumptions are made, while the numerical simulation is more reductive to the actual working conditions and more sufficient to quantify the interference, so the group anchor effect coefficient is smaller. In summary, the difference between the group anchor effect coefficient calculated in this paper and the original method and numerical simulation results is small, which proves the rationality of the theoretical calculation method in this paper.

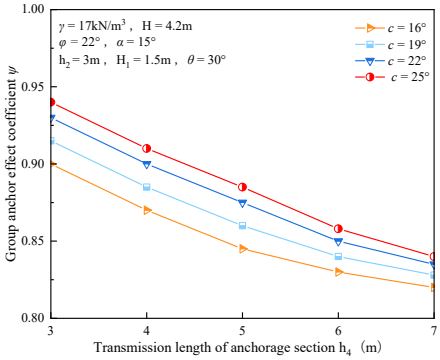
5 Parameter analysis

Because the anchor group effect coefficient is a parameter reflecting the influence of stress superposition on anchorage performance in multi-anchor cable anchorage system, and the stress superposition range is different in different regions, it is necessary to analyze the relevant parameters of anchor group effect coefficient involved in

the corresponding mechanical models of upper layer, lower layer, left side and right side.

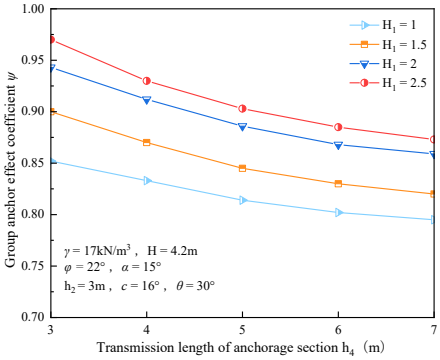
5.1 Parameter analysis of transfer-group anchor effect coefficient of upper layer anchor cable

Figure 9 (a-d) shows the transmission cable layout in the upper layer of the calculation cable, with different influence parameters (soil cohesion c, arrangement spacing H_1, arrangement inclination α, calculated anchor cable anchoring section length h_2), the curve of group anchor effect coefficient ψ varying with the anchor cable anchoring section length h_4 of the transmission anchor cable. From Figure 9 (a-d), it can be seen that the longer the anchor cable anchoring section length h_4 of the transmission anchor cable, the smaller the group anchor effect coefficient ψ, because the overlapping range is expanding and the mutual interference is increasing; Secondly, the larger the length of transfer anchor segment h_4, the gentler the change of group anchor effect coefficient, which is due to the fact that the interference degree tends to be stable when the superposition range of group anchors reaches a certain extent. It can be seen from Figure 9 (a) that when other parameters are fixed, the group anchor effect coefficient ψ increases significantly with the increase of cohesion c, because the larger c, the stronger the integrity of soil, the higher the stress transfer efficiency among group anchors, the higher the group anchor effect coefficient ψ, the smaller the reduction effect on the pullout bearing capacity of single anchor; It can be seen from Figure 9 (b) that when all parameters are fixed, the larger the upper layer anchor cable spacing H_1 is, the larger the group anchor effect coefficient ψ is, and the influence degree is much greater than other parameters, because the anchor cable spacing directly determines the superposition range among group anchors. When the spacing increases to a certain extent, the group anchor effect coefficient ψ gradually approaches 1, and at this time, the group anchor can achieve the pullout bearing performance of single anchor; Figure 9 (c) shows that when other parameters are fixed, anchor effect coefficient ψ decreases slightly with the increase of arrangement inclination α, because vertical stress field superposition effect between adjacent cables is significant, Influence between anchor groups upgrade，As a result, the group anchor effect coefficient psi will slightly decrease, but the difference will not be too large; it can be seen from Figure 9 (d) that the calculated anchor cable anchoring section length h_2 increases, and the group anchor effect coefficient ψ will decrease, because with the increase of the calculated anchor cable anchoring section length h_2, the overlapping area will be wider, and the influence between the group anchors will become greater, and the weakening effect on the calculation of the uplift bearing capacity of the anchor cable will be more obvious, and the group anchor effect coefficient ψ will decrease.



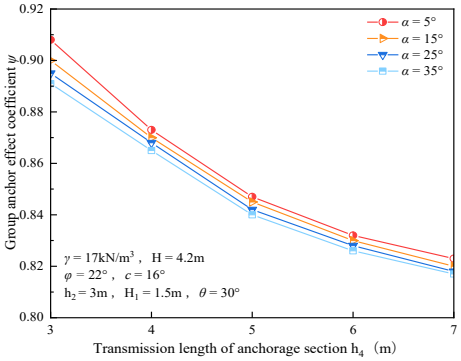
381

382 （a）soil cohesion



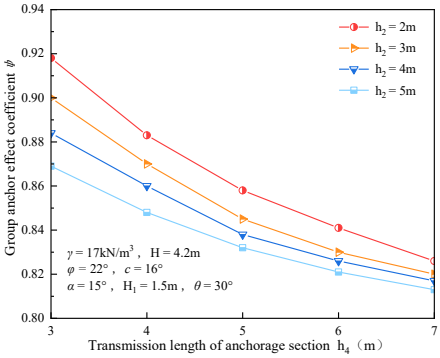
383

384 （b）arrangement pitch



385

386 （c）disposition inclination

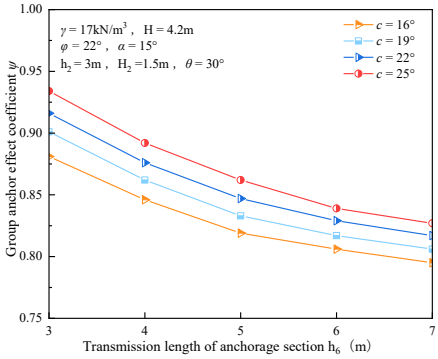


（d）Calculation of anchor length

Fig. 9 Influence of transmission parameters of upper layer anchor cable on group anchor effect coefficient

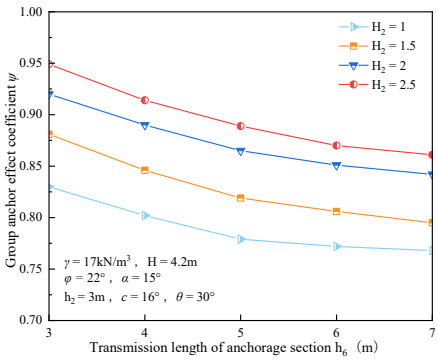
5.2 Parameter analysis of transfer-group anchor effect coefficient of lower layer anchor cable

Figure 10 (a-d) shows the variation law of anchor group effect coefficient ψ with anchor length h_6 of transmission cable under the influence parameters of soil cohesion c, arrangement spacing H_2, arrangement inclination α and anchor length h_2 of calculation cable. Figure 10 (a-d) shows that anchor group effect coefficient ψ shows a decreasing trend with the increase of anchor length h_6 of transmission cable, and the curve gradually tends to be gentle, which is consistent with the analysis conclusion of upper layer anchor cable transmission in 5.1 of this paper. Comparing Figure 9 (a-d) and Figure 10 (a-d), it can be seen that under the same parameter conditions, the variation degree of anchor group effect coefficient caused by lower layer transfer anchor cable is generally greater than that of upper layer transfer anchor cable, which indicates that the weakening effect of lower layer anchor cable on the calculation of anchor cable pull-out bearing capacity is more obvious. This is mainly because the lower layer anchor cable is located in the middle and lower part of the calculation anchor cable fracture cone, and the soil in this area is more likely to reach the shear strength limit, causing local failure, thus leading to anchor cable failure. According to the influence trend of each parameter, when other parameters are constant, the anchor group effect coefficient ψ increases with the increase of cohesion c and lower layer anchor spacing H_2, and decreases with the increase of arrangement inclination α and calculated anchor length h_2.



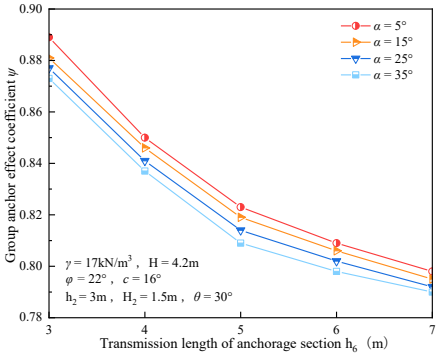
405

406 （a）soil cohesion



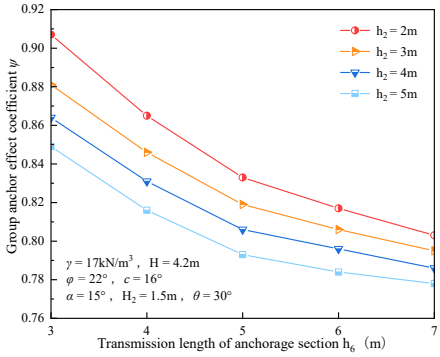
407

408 （b）arrangement pitch



409

410 （c）disposition inclination



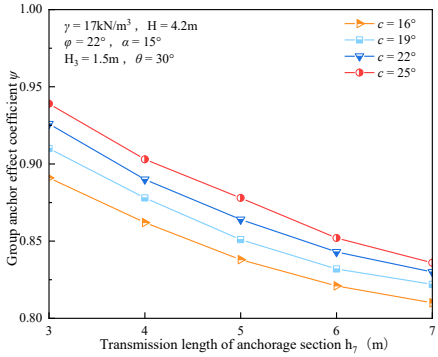
411

412 （d）Calculation of anchor length

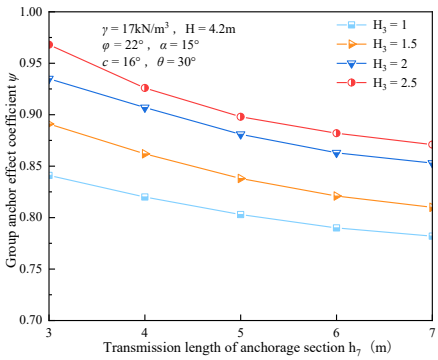
413 Fig. 10 Influence of transmission parameters of lower layer anchor cable on group anchor effect coefficient

414 **5.3 Parameter analysis of transfer-group anchor effect coefficient of left and right anchor cables**

415 Figure 11 (a-b) shows the curve of anchor group effect coefficient ψ varying with anchor length h_7 of
416 transmission anchor cable under the influence parameters of soil cohesion c and arrangement spacing H_3 when
417 transmission anchor cable of recoverable anchor cable is arranged on the right side of calculation anchor cable. It
418 should be noted that in actual engineering, arrangement inclination α of recoverable anchor cable arranged
419 horizontally is generally consistent with anchor length h_2 of calculation anchor cable, so parameter analysis is not
420 conducted. It can be seen from the overall change trend of Figure 11 (a-b) that the anchor group effect coefficient
421 ψ shows a downward trend and the curve gradually tends to be gentle with the increase of the anchor length h_7 of
422 the transfer anchor cable. Compared with Figure 11 (a-b), Figure 10 (a-d) and Figure 9 (a-d), it can be seen that
423 under the same parameter conditions, the change degree of anchor group effect coefficient caused by the right
424 transfer anchor cable is generally smaller than that of the lower transfer anchor cable and larger than that of the
425 upper transfer anchor cable. According to the influence trend of each parameter, when other parameters are
426 constant, the anchor group effect coefficient ψ increases with the increase of cohesion c and the distance H_3
427 between right cables, which is consistent with the analysis law of upper and lower cables, and further confirms
428 that improving soil strength and reasonable control distance have positive effects on eliminating anchor group
429 effect.



（a）soil cohesion



（b）arrangement pitch

Fig. 11 Influence of transmission parameters of right anchor cable on group anchor effect coefficient

6 Conclusion

This paper considers the actual layout conditions of recoverable anchor cables in foundation pit engineering, establishes a group anchor calculation model, and derives the group anchor effect coefficient. The rationality of the proposed calculation method is verified through case study validation and parametric analysis. The main conclusions are as follows:

(1) The anchor effect coefficients calculated by this method are in good agreement with PLAXIS3D numerical simulation and existing theoretical results, and the deviation is between 2.6% and 4.3%. The research results provide reference for the anchor design of recoverable anchor groups.

(2) The anchor group effect coefficient increases with the increase of soil cohesion and cable spacing, and decreases with the increase of cable inclination, calculated anchor length and transmitted anchor length. Among all the influencing factors, the cable spacing has the greatest influence on the anchor group effect. By optimizing

cable spacing, adjusting anchor length and cable inclination, the mutual interference of anchor group can be effectively weakened and the anti-pulling bearing efficiency of supporting structure can be improved.

(3) The influence of transmission cables in different directions is obviously different. The interference effect of transmission cables in lower layers is the strongest, the influence of transmission cables in left and right sides is the second and tends to be similar, and the influence of transmission cables in upper layers is relatively small.

Acknowledgments

This work was supported by the Gansu Provincial Major Science and Technology Special Program (Grant No. 24ZDFA010),and the Gansu Provincial Key Research and Development Program (Grant No. 24YFFA070).

Date Availability Statement Some or all data, models, or code that support the findings of this study are available from the corresponding author upon reasonable request.

Declaration of Competing Interest

The authors declare that they have no known competing financial interests or personal relationships that could have appeared to influence the work reported in this paper.

References：

[1] Menaka K, Mukherjee S, Babu S L G, et al. Reliability Analysis of Micropile-Supported Deep Excavations Using Multivariate Adaptive Regression Splines[J]. Geotechnical and Geological Engineering, 2026, 44(2): 101-101.

[2] Li Y, Ma Z, Gao F, et al. Stability of a Deep Foundation Pit with Hard Surrounding Rocks under Different in-Time Transverse Supporting Conditions[J]. Applied Sciences, 2024, 14(7).

[3] 程雪松, 张润泽, 郑刚, 等. 局部超挖或超载作用下桩锚支护基坑连续垮塌试验研究[J/OL]. 岩土工程学报, 1-11[2024-09-29].

[4] Wu J, Ye S, Wang Z, Y ang D. Application and Automatic Monitoring and Analysis of Hybrid Support Structure in Ultra DEEP Foundation Pit Engineering in the Lan zhou Area under Complex Environmental Conditions[J]. Water. 2023; 15(7): 1335.

[5] 周勇, 朱亚薇. 深基坑桩锚支护结构和土体之间协同作用[J]. 岩土力学, 2018, 39(9): 3246-3252.

[6] Yongshuai S, Zhiming L. Analysis of Deep Foundation Pit Pile-Anchor Supporting System Based on FLAC 3D[J]. Geofluids, 2022.

[7] 叶帅华, 赵壮福, 吴强, 等. 西北黄土地层中可回收钢筋锚杆的锚固性能研究[J]. 地基处理, 2020, 2(3): 196-202.

[8] 叶帅华, 黄义冠, 叶炜钠, 等. 挤压锚式可回收锚索在黄土基坑中的应用[J]. 地基处理, 2023, 5(4): 312-322.

[9] 叶帅华, 吴映坤, 黄安平. 挤压锚式可回收锚索在卵石基坑的回收试验分析[J]. 地基处理, 2022, 4(3): 226-233.

[10] 王哲, 王乔坎, 马少俊, 等. 扩大头可回收预应力锚索极限抗拔力计算方法研究[J]. 岩土力学, 2018, 39(S2): 202-208.

[11] 王建. 可回收式预应力锚索作用机理及施工力学分析[D]. 北京: 北京交通大学, 2009.

[12] Ye S H, Zhang J, Ye W N. Research on Stress Distribution Law of Recoverable Anchor Cable[J]. Soil Mechanics and Foundation Engineering, 2025, 61(6): 1-11.

[13] 吴强. 可回收预应力锚杆（索）作用机理及适用性研究[D]. 兰州: 兰州理工大学, 2021.

[14] 裴亚建. 预应力锚索加固边坡中的群锚效应研究[D]. 重庆: 重庆交通大学, 2020.

[15] 卢瑞娜. 锚杆挡土墙加固时锚固段群锚效应研究[D]. 重庆: 重庆大学, 2013.

[16] 陈晨, 张长轩, 刘哲, 等.连续球体型锚杆群锚效应模型试验研究[J]. 岩土工程学报, 2026, 48(4): 781-792.

[17] 庞有师, 刘汉龙, 柯结伟, 等. 新型可回收锚杆不同布置间距的群锚效应[J]. 河海大学学报(自然科学版), 2009, 37(6): 685-690.

[18] Ghaly Ashraf, Hanna Adel. Model investigation of the performance of single anchors and groups of anchors [J]. Canadian Geotechnical Journal,

1994, 31(2): 168-178

[19] Hanna Adel, Ghaly Ashraf. Ultimate pullout resistance of groups of vertical anchors [J]. Canadian Geotechnical Journal, 1994, 31(5):673-682

[20] 黄宏阳. 深层黏性土中伞型锚锚固体特征与群锚效应研究[D]. 武汉: 长江科学院, 2025.

[21] 乔建刚, 李娟, 张勇, 等. 基于 PFC 的抗浮锚杆上拔群锚效应研究[J]. 辽宁工程技术大学学报(自然科学版), 2025, 44(1): 93-101.

[22] 俞晓, 苏晓科. 基于圆锥体与棱柱体组合破坏面的土层锚杆承载力分析[J]. 结构工程师, 2006, (3): 57-59.

[23] 王兰民. 黄土动力学[M]. 北京: 地震出版社, 2003.

[24] 刘祥沛,董天文,郑颖人.有限元荷载增量法在判定桩基础极限荷载的应用[J].兵器装备工程学报, 2016, 37(5): 144-148+172.